In Silico Comparison of Phase Maps Based on Action Potential and Extracellular Potential

Konstantin Ushenin[1,2], Artem Razumov[1,2], Vitaly Kalinin[3], Olga Solovyova[1,2]

[1] Ural Federal University, Ekaterinburg, Russia
[2] Institute of Immunology and Physiology, Ekaterinburg, Russia
[3] EP Solution SA, Yverdon-les-Bains, Switzerland

Abstract

In this work, a computer simulation of the reentrant ventricular tachycardia (VT) was used to investigate the peculiar properties of phase maps based on transmembrane potentials (TP) and extracellular potentials (EP). The simulation approach included the bidomain model with full myocardium-torso coupling, a realistic ionic model of the human cardiomyocytes and a personalized geometry of the heart and torso. The phase mapping pipeline includes a signal detrending and the Hilbert transform. It was demonstrated that TP-based phase maps correlated well with the propagation of cardiac excitation. In contrast, EP-based phase mapping provides some aberrations which can complicate electrophysiological interpretation of the phase maps in terms of cardiac activation sequence. It was also shown that a modification of the phase computation algorithm, including the sign inversion of signals and a special transformation of the phase plot, can partially eliminate these aberrations and make EP-based phase maps resemble TP-based maps.

1. Introduction

Phase mapping is a widely used approach for signal processing and visualization of reentrant activity in the heart. Initially, the phase mapping was developed to process transmembrane potential (TP) signals that were recorded in ex-vivo optical mapping of the heart [1]. However, the TP recording is challenging in humans, and the phase mapping approach was adapted to work with extracellular electrical potential (EP) signals (unipolar electrograms) [2].

This adaptation requires a modification of the phase mapping algorithm because TP and EP signals have different morphologies and electrophysiological natures. In recent works [3, 4], several updates of the phase mapping algorithm have been proposed in order to make TP-based phase maps more appropriate for the diagnosis of cardiac arrhythmias. However, the problem of an optimal EP-based phase mapping algorithm remains to be solved.

In our study, we use a detailed computer model of reentrant activity in the human ventricles to study the difference between phase maps based on TP and EP, and propose a modified version of the algorithm for EP-based phase mapping which makes EP-based phase maps more resemble to TP-based ones.

2. Methods

2.1. Electrophysiology model

The simulation approach was described in our previous work [5]. Briefly, personalized geometry model of the human heart and torso were created using computed tomography data of a patient with the dilated cardiomyopathy. The segmentation and the meshing were performed by Amycard 01 K system (EP solutions SA) and GMSH open source software, respectively. Myocardial anisotropy was determined using the rule-based approach. The bidomain model with full myocardium-torso coupling and a TNNP model of the human heart ventricular cardiomyocytes [6] was used. Transmural heterogeneity was introduced discretely as the epicardial and endocardial layer with a ratio of 50:50. Apicobasal heterogeneity was introduced by linear changes of g_{Ks} conductivity from the apex to the base. A reentrant process that served as an in-silico model of polymorphic VT was induced by the virtual pacing using the S1S2 protocol. The tachycardia cycle was 240-260 ms. The core of the single electrical rotor drifted within a region of 5 cm in diameter in the lateral wall of the left ventricle. The simulation provided TP signals and EP signals (local unipolar electrograms) in each node of the cardiac model. The signals at the time interval from 1650 ms to 3000 ms were selected for the phase processing.

2.2. Phase mapping

The general pipeline for the phase processing of the TP and EP signals included band-pass filtering with $1 - 250$

 ISSN: 2325-887X DOI: 10.22489/CinC.2018.172

Hz bandpass, signal detrending, and the normalization of the signals to the range [-1,1], the calculation of instantaneous phase angles and a visualization of the results on the myocardium surface. Detrending and the normalization of the signals performed by the method, proposed in [7]; the method is based on the determination of the bounds of the signals by the upper and lower splines passing through the signal minimal and maximal peaks. Real values TP and EP signals V_k^t and ϕ_k^t were complemented to analytical signals $V_k^t + iH[V_k]^t$ and $\phi_k^t + iH[\phi_k]^t$, respectively, by the Hilbert transform. Next, the phase angles were calculated according to the formulas:

$$\text{TP}_k^t = \text{arctan2}(V_k^t, H[V_k^t]), \quad (1)$$

$$\text{EP}_k^t = \text{arctan2}(\phi_k^t, H[\phi_k^t]) \quad (2)$$

where TP_i^t, EP_i^t are phase angle of the TP and EP signals, respectively. These phase angle definitions are referred to as the basic methods.

In this paper, we also proposed a modified method for the calculation of the EP signal phases. The method included the inversion of the sign of EP signals and a shift of the phase plane origin on some vectors:

$$\text{EP}_k^t = \text{arctan2}(-\phi_k^t - \alpha, H[-\phi_k^t] - \beta) \quad (3)$$

The algorithm for the calculation of vector (α, β) is proposed below.

2.3. Calculation of Phase Plane Origin Shift

Fig. 1(a) shows the phase planes with the TP and EP analytical signals from 1000 random points on the model. There are several analytical signals that do not encircle the phase plane origin. The proposed algorithm searches a point that is encircled by a greater number of analytical signal loops that the initial phase plane origin.

The main idea is to build a two-dimensional histogram with the density of all analytical signals on the discretized phase plane. The sequential values of an analytical signal may be placed at a relatively large distance because of the signal discretization step. This forces us to present each analytical signal as the polyline and use its points for histogram construction.

Several polylines could pass through the same points on the discretized phase plane. Let us denote the natural logarithm from the number of lines that pass through one point as lines per point (LPP) value. The application of the logarithm is suitable here because some points have very high LPP values.

The first part of the algorithm builds an discrete phase plane M with LPP values. The input signals are denoted as S_k^t, $k = 0..N$, $t = 0..T$. The discrete phase plane is

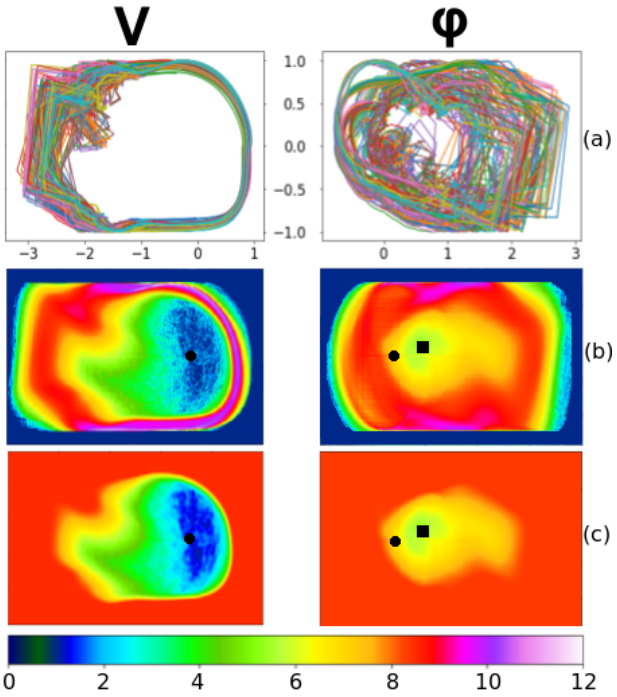

Figure 1. (a) 1000 analytical signals plotted on the same phase plane. (b) All analytical signals are plotted on the discrete phase plane M by polylines (logarithmic scale). (c) LPP values for TP and EP phase maps after M post-processing. A black circle is an initial phase plane origin. A black square is a phase plane origin proposed by the algorithm.

a matrix $i = 1..n, j = 1..m : M_{i,j} = 0$. A function $f : (x+iy) -> ([\rho x + \frac{n}{2} + 1], [\rho y + \frac{m}{2} + 1])$ transforms the complex number $x+iy$ into a pair of the natural matrix indexes $(a, b) = ([\rho x + \frac{n}{2} + 1], [\rho y + \frac{m}{2} + 1])$, $a, b \in \mathbb{N}$, where $\rho = 10^p$ is the transformation precision, and [] is the rounding operator.

Each analytical signal is presented as a polyline. Bresenham's algorithm transforms each segment of that polyline into the set of points, which are drawn on the M.

for $k \leftarrow 0..N$ **do**:
  $\{P\}_{j=1}^T \leftarrow \text{Polyline}(f, S_k^t)$
  for P **in** $\{P\}_{j=1}^T$ **do**:
    $\{(a,b)\}_{k=1}^K \leftarrow \text{Bresenham}(P_k)$
    for (a,b) **in** $\{(a,b)\}_{k=1}^K$ **do**:
      $M_{a,b} \leftarrow M_{a,b} + 1$

The results of these processing are shown in Fig.1(b).

The following matrix M processing was performed with the goal to making M more suitable for visualization and to remove the region that is close to the M border from our consideration. It includes the logarithm transformation of all values (**for** $i = 1..n, j = 1..m : M_{i,j} \leftarrow \ln(M_{i,j})$), and the application of smoothing and morphological oper-

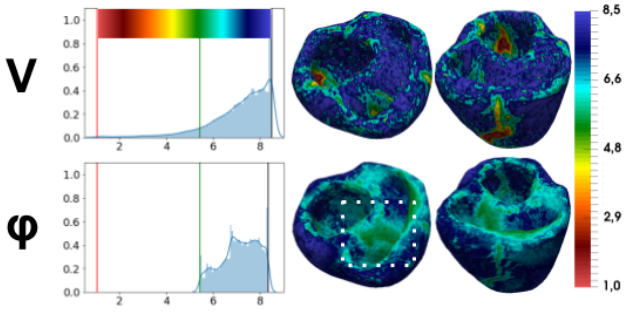

Figure 2. The minimal LPP value distribution and map of the LPP value on the myocardium surface

ations to M: gaussian smoothing with σ, and filling border region by h value. The result of this processing is shown in Fig. 1(c). The values of $M_{i,j}$ are lines per point (LPP) values that were defined above.

Next, the threshold cutting with level g was performed on M. Thus, we obtain the region in the center of M which was encircled by the main part of all the analytical signals. The center of mass for this region (α, β) is the new phase plane origin proposed by the algorithm.

Finally, each polyline was analyzed again to determine the minimal LPP value for each signal source and to keep it in vector $L_k \leftarrow \min_{(a,b)\in\{\{(a,b)\}_{k=1}^{K}\}_{j=1}^{T}} M_{a,b}$.

Point (α, β) and vector L_k are the algorithm output values.

3. Results

The phase signals and 3D phase maps that were calculated using the formulas (1) and (2), (3) were compared to each other and to the TM signals and maps. This analysis was focused on a location of the phase fronts on the model surface and the position of the phase breaks (from $-\pi$ to π or from π to $-\pi$) on the timeline.

The proposed algorithm was applied to the TP and EP signals with the following parameters: $\rho = 10^2 = 100$, $h = 8.5$. The matrix with LLP values based on TP had a large free region, including the phase plane origin under low threshold level $g = 0.1$. The matrix with the LLP values for EP had a small region with a center

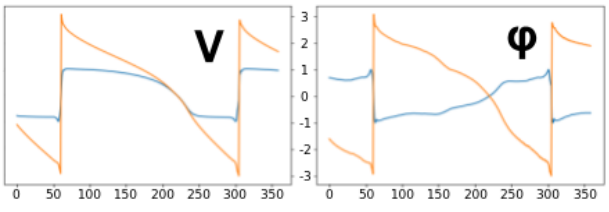

Figure 3. Normalized TP and EP with their phase angle values.

$(\alpha, \beta) = (-0.15, 0.5)$, and was filled by a notable number of analytical signals, under $g = 4$. The proposed phase plane origin shift increases the number of loops, encircling the phase plane origin.

The statistical distributions of LPP minimal values for each signal source and their representations on the model surface are shown in Fig. 2. The statistical distributions for the TP and EP signals were different, but the similar spatial regularities of LPP minimal values could be traced in both cases: the minimal values of this index were observed in the regions of the rotor core. Also, the region with relatively small minimal the LPP values were located in septum for EP processing. In these results, we expected phase map aberrations.

An example of the TP phase angle values as well as an EP phase angle values that were computed using formulas (1) and (3) are presented in Fig. 3. Maps for each phase angle definition on the myocardium surface are shown in Fig. 4. The phase break of the TP phase signals matched the upstroke of action potentials, namely at the moments of the myocardium activation. The mean difference between the phase break and the activation times was 1-3 ms. In contrast, phase breaks of the EP phase signals that were computed using formula (2) were not well matched with a TP upstroke.

Usage of the original phase origin without the (α, β) shift for the phase angle computation led to an abberation of the phase maps on the model surface. An example of TP based and EP based 3D phase maps are presented in Fig. 4. In contrast to the TP based phase maps, the EP based phase maps that were created without the phase plane origin shift have some aberrations that are shown in Fig. 4(e). In particular, there was an observed false phase front (i.e. the front that did not correspond to the front of myocardial depolarization). The application of the shift to phase angle definition (3) made EP-based phase maps more similar to TP-based maps and reduced their aberrations.

4. Discussion and Conclusion

Phase mapping is mainly used for detecting and tracking electrophysiological rotor cores based on the calculation of so-called phase singularities. Nevertheless, the interpretation of phase maps in terms of a cardiac activation sequence can be useful for the diagnosis of cardiac arrhythmia. The results of this study show that TP based phase maps can provide information about the dynamics of myocardial activation. However, EP based phase maps have aberrations that complicate their analysis.

Using formulas (1) and (3) match the TP upstroke with the phase front of the TP based phase map and match the EP downstroke with the phase front of the EP based phase map.

Some analytical signal loops may not encircle the ori-

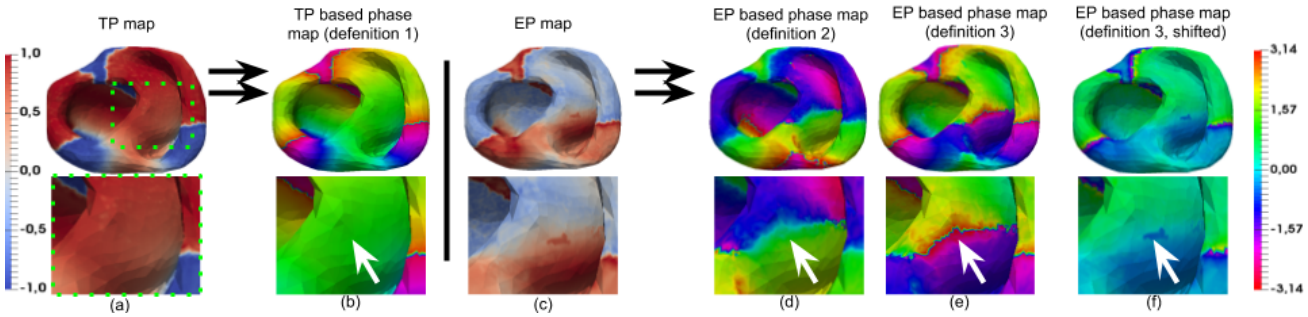

Figure 4. Visualization of results at $t = 2000$ ms. (a) TP map. (b) Phase map based on TP. (c) EP map. (d) Phase map based on EP with abberations. (e) Fixed phase map based on EP.

gin of the phase plots because of the significant variability of the electrogram shape and amplitude. This issue led to some aberrations on the EP based phase maps which complicated their analysis.

Our preliminary in-silico experiments show that the modification of the phase mapping algorithm, including the shift of the phase plane origin, could reduce the number of these aberrations.

Finally, the LPP index was introduced. We belive that the index may be useful for an analysis of phase mapping algorithms, and that it is also a useful tool for phase maps interpretation.

Acknowledgements

The reported study was funded by RFBR according to the research project No. 18-31-00401. Development of computer model with personalized geometry was funded by IIP UrB RAS theme No AAAA-A18-118020590031-8, RF Government Act #211 of March 16, 2013 (agreement 02.A03.21.0006), Program of the Presidium RAS #27 (project AAAA-A18-118020590030-1).

References

[1] Gray R, Pertsov A, Jalife J. Spatial and temporal organization during cardiac fibrillation. NATURE MAR 5 1998; 392(6671):75–78.

[2] Clayton RH, Nash MP. Analysis of cardiac fibrillation using phase mapping. Cardiac electrophysiology clinics 2015; 7(1):49–58.

[3] Kuklik P, Zeemering S, Maesen B, Maessen J, Crijns HJ, Verheule S, Ganesan AN, Schotten U. Reconstruction of instantaneous phase of unipolar atrial contact electrogram using a concept of sinusoidal recomposition and hilbert transform. IEEE transactions on biomedical engineering 2015; 62(1):296–302.

[4] Vijayakumar R, Vasireddi SK, Cuculich PS, Faddis MN, Rudy Y. Methodology considerations in phase mapping of human cardiac arrhythmias. Circulation Arrhythmia and Electrophysiology 2016;9(11):e004409.

[5] Ushenin K, Dokuchaev A, Magomedova S, Sopov O, Kalinin V, Solovyova O. Role of myocardial properties and pacing lead location on ecg in personalized paced heart models. Computing in Cardiology 2017;44:1–4.

[6] Ten Tusscher KH, Panfilov AV. Alternans and spiral breakup in a human ventricular tissue model. American Journal of Physiology Heart and Circulatory Physiology 2006; 291(3):H1088–H1100.

[7] Roney CH, Cantwell CD, Qureshi NA, Chowdhury RA, Dupont E, Lim PB, Vigmond EJ, Tweedy JH, Ng FS, Peters NS. Rotor tracking using phase of electrograms recorded during atrial fibrillation. Annals of biomedical engineering Apr. 2017;45(4):910–923.

Address for correspondence:

Ushenin Konstantin Sergeevich
Ural Federal University
620002, 19 Mira street, Ekaterinburg, Russia
konstantin.ushenin@urfu.ru